

Kinetic-equation approach to nonequilibrium superconductivity*†

Jhy-Jiun Chang and D. J. Scalapino

Department of Physics, University of California, Santa Barbara, California 93106

(Received 26 July 1976)

We have studied thin films driven out of equilibrium under spatially uniform steady-state conditions by thermal phonon injection, microwave and optical irradiations, and quasiparticle tunneling injection. The linearized coupled kinetic equations for the quasiparticle and phonon distributions were solved numerically. Results for the change in the energy distributions of quasiparticles and phonons are given for a variety of nonequilibrium situations. Using these distributions, the changes in the ultrasonic attenuation, electrical conductivity and the superconductor-insulator-superconductor tunneling $I(V)$ characteristic in various nonequilibrium states are obtained.

I. INTRODUCTION

Nonequilibrium states of a superconducting thin film can be created by injecting electrons, photons, or phonons into the thin film. More than a decade ago, Ginsberg¹ used a double tunnel junction in an attempt to measure the recombination lifetime of the quasiparticles in the superconducting thin film which formed part of the junction. Modified techniques were developed later.²⁻⁷ In these experiments, the superconductors were driven out of equilibrium by the bias voltage on one of the junctions, and the change in the $I(V)$ characteristics were detected to give information about the quasiparticle recombination time. New structures which appeared in the $I(V)$ characteristic of the detector junction⁶⁻¹⁵ and the energy spectrum of the phonons emitted by the nonequilibrium thin film have been investigated.¹¹⁻¹³

Wyatt *et al.*¹⁶ and Dayem and Wiegand¹⁷ studied a superconducting microbridge irradiated by microwaves and found that the critical current could be enhanced by the microwaves. Recently this effect has been further investigated by other groups.¹⁸

Dynes and Narayanamurti^{13,19} studied superconductors pumped by heat pulses and showed that superconductors could be used as phonon detectors and phonon energy converters for phonons of energy about twice the gap energy Δ of the superconductor. Tredwell and Jacobsen²⁰ investigated superconductors injected with monochromatic phonons of frequency $\Omega < 2\Delta/\hbar$. They found a more profound enhancement in the critical current than that obtained by microwave irradiation.^{16,17}

Testardi²¹ observed a resistive state in a superconducting thin film which was irradiated by a laser. This resistive state begins to occur at a temperature below the usual transition temperature T_c and could not be explained simply in terms of heating. This interesting result stimulated a

series of investigations on superconducting thin films driven out of equilibrium by laser irradiation. Parker and Williams²² and Hu *et al.*²³ studied the $I(V)$ characteristics of laser irradiated tunnel junctions, and Sai-Halasz *et al.*²⁴ and Janik *et al.*²⁵ studied the microwave response of laser irradiated thin films.

Several theoretical models have been developed to analyze the data and to explain the results of experiments on nonequilibrium superconducting systems. At an early stage of the quasiparticle recombination time measurement, Rothwarf and Taylor²⁶ proposed two coupled equations (henceforth referred to as RT equations) to relate the quasiparticle recombination time observed from the tunneling measurement to the average intrinsic quasiparticle recombination time. They pointed out that in real experimental situations, the phonons produced from quasiparticle recombination have a high probability of being absorbed in a pair-breaking process before they can escape from the sample. This is known as the phonon-trapping effect and can lead to an observed recombination lifetime much longer than the intrinsic lifetime. However, their coupled equations govern only the macroscopic quasiparticles and phonon densities and do not give the energy distributions of these excitations.

Eliashberg²⁷ and Ivlev *et al.*²⁸ used a quasiparticle kinetic equation to study the energy gap enhancement in a microbridge by microwave irradiation. Tredwell and Jacobsen²⁰ used the same model to explain the critical-current enhancement due to the monochromatic phonon injection. In their studies, the phonons were assumed to be in thermal equilibrium with the ambient temperature and hence, the phonon-trapping effect was ignored. Dayem and Wiegand¹² used a discrete-level model for the quasiparticle and phonon states to discuss the energy spectra of phonons emitted from a nonequilibrium superconductor. In their investigation,

they required detailed balances of the phonon scattering as well as the phonon pair-breaking process.

As for the theories dealing with superconductors irradiated by optical radiation, Vardanyan and Ivlev²⁹ used a model which ignores the phonon trapping effect. Scalapino *et al.*^{30,31} and Parker³² proposed models based upon the assumptions that scattering processes are the dominant relaxation mechanism while the quasiparticle recombination processes and the phonon pair-breaking processes, respectively, form the bottleneck.

Recently, Kaplan *et al.*³³ have made detailed calculations of the quasiparticle and phonon lifetimes for equilibrium superconductors. The temperature and energy dependences of these lifetimes were studied. Their results indicate that in a nonequilibrium superconductor, the quasiparticle scattering and recombination processes have to be treated on an equal footing. Furthermore, because of the short-phonon pair-breaking lifetime, the phonon-trapping effect is always important.

In this article we study the steady-state quasiparticle and phonon distributions for a superconducting thin film driven out of equilibrium. We begin with the coupled quasiparticle and phonon kinetic equations³⁴ and the BCS gap equation^{27,35} with a modified quasiparticle distribution function. These coupled equations govern the energy distributions of quasiparticle and phonon excitations and take into account the temperature and frequency dependences of the electron-phonon interaction cross sections. The phonon-trapping effect is treated by introducing a phonon escape time τ_{es} into the phonon kinetic equation. This escape time, in general, depends upon the thickness of the thin film and the acoustic match between the film and its environment and is an intrinsic property of the sample geometry and substrate. It should also depend upon the energy of the phonon which passes the boundary of the film. For simplicity we assume a uniform steady state for the nonequilibrium superconducting thin film and use an energy- and space-independent constant for the phonon escape time. Since the phonon energy of interest is of order a few times the gap energy or less, which is small compared with the Debye energy, it is justifiable to use an energy-independent escape time. In order for the film to be uniformly excited, it must be thin compared with the quasiparticle diffusion length. In addition, the level of excitation must not exceed the threshold at which the system becomes unstable. It has been suggested that this instability leads to a driven mixed state.^{23-25,31} Here we are interested in the properties of the more weakly driven homogeneous nonequilibrium states. We report here results for

the quasiparticle and phonon distributions obtained from the linearized coupled kinetic equations and relegate the investigation of the full nonlinear equations to future study.

We consider superconducting thin films driven out of equilibrium by (a) thermal phonon injection, (b) microwave irradiation, (c) quasiparticle injection through a normal-insulator-superconductor (NIS) tunnel junction, and (d) optical irradiation. The first three cases involve only low-energy excitations of quasiparticles and phonons and serve, respectively, as prototypes of phonon, microwave, and electron injections as driving mechanisms. In case (d), optical photons can excite electrons into high-energy states which are significantly broadened by their short lifetimes. Furthermore, electron-electron interactions as well as electron-phonon interactions can be important for the decay of quasiparticles in these high-energy states. Therefore, additional care has to be exercised before the coupled kinetic equations, which ignored the electron-electron interactions, can be applied to such a nonequilibrium system.

We have also investigated the transport properties of the driven films using the calculated steady-state quasiparticle distributions. These properties include the ultrasonic attenuation coefficient, the dynamic electric conductivity and the current-voltage characteristic of a superconductor-insulator-superconductor (SIS) tunnel junction involving nonequilibrium superconductors. These transport properties are not only interesting in themselves, but they provide useful probes for the understanding of the nonequilibrium state. Recently, the authors³⁶ have shown that the quasiparticle distribution function at the gap edge as well as the quasiparticle density in the superconductor can be directly determined from the $I(V)$ characteristic. Furthermore, the steady-state quasiparticle distribution can be related to the $I(V)$ characteristic by a linear integral equation and hence, in principle, can be unfolded from the experimentally determined $I(V)$ curve. Similar results are found for the ultrasonic attenuation coefficient and the dynamic conductivity.

The layout for the rest of the article is as follows: In Sec. II we discuss the coupled kinetic equations. In Sec. III we present the numerical solutions of the quasiparticle and phonon distributions obtained from the linearized coupled kinetic equations. The physical origin of the structures in these distributions will be discussed. This section is followed by the study of the transport properties using the calculated quasiparticle distribution functions. Finally, in Sec. V we summarize our important findings and give some brief concluding remarks. In Appendix A we study the connection between the

Rothwarf-Taylor equations and the kinetic equations. Appendix B contains a discussion of the linearized form of the Rothwarf-Taylor equations.

II. COUPLED KINETIC EQUATIONS

In order to discuss the kinetic equations, it is necessary to understand the various relaxation processes for quasiparticles, phonons, and the gap parameter Δ . It is well known that for the phonons and low-energy quasiparticles of energy $E < \hbar\omega_D$, where $\hbar\omega_D$ is the phonon Debye energy, the relaxations are mainly due to the electron-phonon interactions which may or may not involve paired electrons.³⁷ These relaxation processes are shown in Fig. 1. The diagram shown in Fig. 1(a) represents the basic electron-phonon scattering process. In terms of the quasiparticle relaxation, it can be read as the decay of a quasiparticle of energy E into a state of energy $(E - \hbar\Omega)$ with the emission of a phonon of energy $\hbar\Omega$. When all the arrows in Fig. 1(a) are reversed, the diagram can be considered as an event creating a quasiparticle of energy E due to the absorption of a phonon by a quasiparticle in a lower-energy state. Since the phonon distribution changes when this scattering process occurs, this process can also be considered as a relaxation process for phonons and contributes to the phonon-scattering lifetime. The quasiparticle recombination process is shown in Fig. 1(b). Here a quasiparticle of energy E combines with another quasiparticle into a pair state and emits a phonon of energy $\hbar\Omega \geq 2\Delta$. Again when all the arrows are reversed, this can be considered as a quasiparticle creation process due to pair breaking by a phonon of energy $\hbar\Omega \geq 2\Delta$. In terms of phonon relaxation, this represents a phonon pair-breaking process. A complete investigation of the quasiparticle and phonon lifetimes for equilibrium superconductors associated with

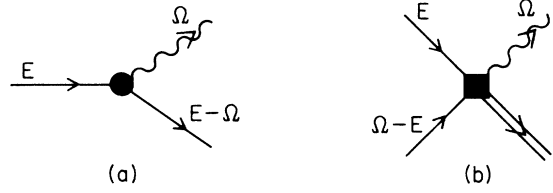


FIG. 1. Relaxation processes for phonons and quasiparticles, (a) the scattering process and (b) the recombination process in which paired electrons are involved.

these processes as well as that corresponding to the branch mixing^{15,38} are given in Ref. 33. For a nonequilibrium superconductor, the quasiparticle and phonon distributions as well as the energy gap are different from their equilibrium values. Since these lifetimes depend upon the quasiparticle and phonon distributions, their values vary, in general, for different driving mechanisms and for different strengths of the driving forces.

In our present work we will be interested in superconducting states which can be described by a nonequilibrium mean-field-pairing amplitude. Thus, we will be treating systems away from the immediate vicinity of the critical point so that the pair-field relaxation time will be short compared to the quasiparticle and phonon relaxation times.³⁹ With the quasiparticle and phonon relaxation process discussed above taken into account, Bardeen, *et al.*³⁴ have derived from Fermi's golden rule the coupled quasiparticle and phonon kinetic equations. Using Green's-function techniques Prange and Kadanoff⁴⁰ have derived similar kinetic equations appropriate for strong coupling electron-phonon systems. Here the momentum dependence is integrated out leaving distributions which depend only upon energy. After the interaction vertices are replaced by the effective electron phonon coupling $\alpha^2(\Omega)$,⁴¹ the coupled equations can be written in the following form:

$$\begin{aligned} \frac{df(E)}{dt} = & I_{qp}(E) - \frac{2\pi}{\hbar} \int_0^\infty d\Omega \alpha^2(\Omega) F(\Omega) \rho(E + \Omega) \left(1 - \frac{\Delta^2}{E(E + \Omega)}\right) \{f(E)[1 - f(E + \Omega)]n(\Omega) - f(E + \Omega)[1 - f(E)][n(\Omega) + 1]\} \\ & - \frac{2\pi}{\hbar} \int_0^{E-\Delta} d\Omega \alpha^2(\Omega) F(\Omega) \rho(E - \Omega) \left(1 - \frac{\Delta^2}{E(E - \Omega)}\right) \{f(E)[1 - f(E - \Omega)][n(\Omega) + 1] - [1 - f(E)]f(E - \Omega)n(\Omega)\} \\ & - \frac{2\pi}{\hbar} \int_{E+\Delta}^\infty d\Omega \alpha^2(\Omega) F(\Omega) \rho(\Omega - E) \left(1 + \frac{\Delta^2}{E(\Omega - E)}\right) \{f(E)f(\Omega - E)[n(\Omega) + 1] - [1 - f(E)][1 - f(\Omega - E)]n(\Omega)\} \end{aligned} \quad (1a)$$

and

$$\begin{aligned} \frac{dn(\Omega)}{dt} = & I_{ph}(\Omega) - \frac{8\pi}{\hbar} \frac{N(0)}{N} \int_\Delta^\infty dE \int_\Delta^\infty dE' \alpha^2(\Omega) \rho(E) \rho(E') \\ & \times \left\{ (1 - \Delta^2/EE') \{f(E)[1 - f(E')]n(\Omega) - f(E')[1 - f(E)][n(\Omega) + 1]\} \delta(E + \Omega - E') \right. \\ & \left. - \frac{1}{2}(1 + \Delta^2/EE') \{[1 - f(E)][1 - f(E')]n(\Omega) - f(E)f(E')[n(\Omega) + 1]\} \delta(E + E' - \Omega) \right\}. \end{aligned} \quad (1b)$$

Here $f(E)$ and $n(\Omega)$ are, respectively, the steady-state quasiparticle and phonon distributions. The driving terms $I_{qp}(E)$ and $I_{ph}(\Omega)$ are, respectively, the quasiparticle and phonon injection rates. The first (second) integral term in Eq. (1a) is contributed by the scattering of a quasiparticle of energy E by the absorption (emission) of a phonon. The third integral term comes from the quasiparticle recombination process. Similarly, in Eq. (1b), the first term in the bold parentheses is due to the phonon scattering process, while the second term comes from the phonon pair-breaking process. These are easily recognized by examining the coherence factors and the electron and phonon distribution functions. The function $\rho(E)$ is the normalized quasiparticle density of states given by

$$\rho(E) = [E/(E^2 - \Delta^2)^{1/2}] \theta(E - \Delta). \quad (2)$$

N is the number of ions per unit volume, $N(0)$ the usual single-spin band and Coulomb-dressed electron density of states at the Fermi energy, and $F(\Omega)$ is the phonon density of states per ion. To calculate the steady-state quasiparticle and phonon distributions one needs to know $\alpha^2(\Omega)F(\Omega)$ and $\alpha^2(\Omega)$. In principle, $F(\Omega)$ can be obtained from neutron-scattering measurements⁴² and $\alpha^2(\Omega)F(\Omega)$ can be obtained from electron-tunneling measurements,⁴³ therefore $\alpha^2(\Omega)$ can be calculated. Here we use a Debye model⁴⁴ for the phonons so that

$$F(\Omega) = \begin{cases} a\Omega^2 & \text{for } \Omega \leq \omega_D \\ 0 & \text{for } \Omega > \omega_D \end{cases} \quad (3)$$

and assume that

$$\alpha^2(\Omega)F(\Omega) = \begin{cases} b\Omega^2 & \text{for } \Omega \leq \omega_D \\ 0 & \text{for } \Omega > \omega_D \end{cases}, \quad (4)$$

where a and b are constants independent of phonon energy. The quadratic dependences of $F(\Omega)$ and $\alpha^2F(\Omega)$ upon the phonon energy are good for low-energy excitations in weak superconductors. For high-energy excitations and/or strong-coupling superconductors, $F(\Omega)$ and $\alpha^2F(\Omega)$ given by expressions (3) and (4) have to be modified. However, we believe that the effects of strong-coupling superconductivity will not have a significant qualitative effect on our result, and as demonstrated later, the accurate energy dependences of $\alpha^2(\Omega)F(\Omega)$ and $F(\Omega)$ in the high-energy region ($\Omega \gg \Delta$) are not necessary for obtaining the non-equilibrium state because of the short lifetimes associated with the states in this region.

Equation (1a) has also been derived by Eliashberg²⁷ using the Green's-function technique with the assumption that the phonons are assumed to

be in equilibrium at the ambient temperature. In the same framework, it is found that the energy gap obeys the same gap equation as for the equilibrium state except for the replacement of the Fermi distribution function by the steady-state quasiparticle distribution function. More generally, as long as the system is outside the immediate vicinity of T_c , the pair field relaxation time is short relative to the quasiparticle and phonon relaxation times, and the steady-state gap parameter Δ satisfies

$$\frac{1}{|\lambda|} = \int_{\Delta}^{\omega_D} dE \frac{1 - 2f(E)}{(E^2 - \Delta^2)^{1/2}}, \quad (5)$$

where λ is the effective strength of the electron-phonon coupling.³⁵

As discussed in the Introduction, in addition to the scattering and recombination processes, a phonon can "decay" by escaping from the thin film. In order to take this into account we add a term

$$[n(\Omega) - n(\Omega, T)]/\tau_{es} \quad (6)$$

to the right-hand side of Eq. (1b). Here $n(\Omega, T) = (e^{\Omega/T} - 1)^{-1}$ is the equilibrium phonon distribution at temperature T . As previously noted, we will neglect the energy dependence of τ_{es} . For the extreme case of $\tau_{es} = 0$, phonons are in equilibrium and we have only to consider Eq. (1a) for the quasiparticle distribution. This is the case considered by Eliashberg²⁷ and Vardanyan *et al.*³⁰ in their studies of superconducting thin films irradiated by microwave and laser radiation. However, as shown in Sec. III, when τ_{es} is of the same order as the phonon pair-breaking time, the phonon-trapping effect cannot be neglected and phonons cannot be considered as being in thermal equilibrium. With expression (6) added to the right-hand side of Eq. (1b), Eqs. (1)–(5) form the basis of our investigation of the distribution functions $f(E)$, $n(\Omega)$, and the gap Δ .

Since the RT equations have been widely applied to the double-junction tunneling measurements as well as the laser-irradiation experiments, it is desirable to make connection between the macroscopic RT equations and the microscopic kinetic equations [Eqs. (1)]. This is given in Appendix A.

Next, we derive the linearized coupled kinetic equations which are to be solved numerically. We define

$$\delta f(E) \equiv f(E) - f(E, T) \quad (7a)$$

and

$$\delta n(\Omega) \equiv n(\Omega) - n(\Omega, T), \quad (7b)$$

where $f(E, T)$ is the Fermi distribution for the

quasiparticles in an equilibrium superconductor at temperature T . [Through this article we use $f(E)$ and $n(\Omega)$ for the steady-state quasiparticle and phonon distributions; the equilibrium distributions are represented by $f(E, T)$ and $n(\Omega, T)$.] Using Eq. (7), the lowest-order terms in Eqs. (1a) and (1b) cancel out completely. We point out that this cancellation is not due to detailed balance in the thermal equilibrium state, because the gap involved is the steady state gap Δ rather than the thermal equilibrium energy gap $\Delta(T)$. Keeping only the first-order terms, we have for the linearized equations

$$\begin{aligned} \frac{d}{dt} \delta f(E) &= I_{qp}(E) - \frac{\delta f(E)}{\tau_{qp}(E, T)} \\ &+ \int_{\Delta}^{\infty} dE' \delta f(E') K_1(E, E'; T) \\ &+ \int_0^{\infty} d\Omega \delta n(\Omega) K_2(E, \Omega; T) \end{aligned} \quad (8a)$$

and

$$\begin{aligned} \frac{d}{dt} \delta n(\Omega) &= I_{ph}(\Omega) - \frac{\delta n(\Omega)}{\tau_{ph}(\Omega, T)} \\ &+ \int_{\Delta}^{\infty} dE \delta f(E) K_3(\Omega, E; T). \end{aligned} \quad (8b)$$

The kernels are given by

$$\begin{aligned} K_1(E, E'; T) &= K_1'(E, E'; T) - K_1'(-E, -E'; T) \\ &+ K_1'(E, -E'; T), \end{aligned} \quad (9)$$

with

$$\begin{aligned} K_1'(E, E'; T) &= (2\pi/\hbar) \alpha^2 F(E - E') \rho(E') (1 - \Delta^2/EE') \\ &\times [f(E, T) + n(E - E', T)] \theta(E - E'); \end{aligned} \quad (9a)$$

$$\begin{aligned} K_2(E, \Omega; T) &= K_2'(E, \Omega; T) + K_2'(-E, -\Omega; T) \\ &+ K_2'(E, -\Omega; T), \end{aligned} \quad (10)$$

with

$$\delta \Delta = \Delta(T) \left[\int_{\Delta(T)}^{\infty} dE \frac{2\delta f(E)}{[E^2 - \Delta^2(T)]^{1/2}} / \left(1 + \int_{\Delta(T)}^{\infty} dE \frac{E}{[E^2 - \Delta^2(T)]^{1/2}} \frac{\partial f(E, T)}{\partial E} \right) \right]. \quad (14)$$

Therefore the change in the energy gap can be calculated as soon as $\delta f(E)$ is obtained from Eq. (8).

III. NUMERICAL SOLUTIONS AND DISCUSSIONS

In this section we discuss the numerical solutions of Eq. (8) for a superconducting thin film in various nonequilibrium steady states. We will study the quasiparticle and phonon distributions and the change in the gap parameter for a non-

$$\begin{aligned} K_2'(E, \Omega; T) &= (2\pi/\hbar) \alpha^2 F(|\Omega|) \rho(E - \Omega) [1 - \Delta^2/E(E - \Omega)] \\ &\times [f(E - \Omega) - f(E)] \theta(E - \Delta - \Omega); \end{aligned} \quad (10a)$$

and

$$\begin{aligned} K_3(\Omega, E; T) &= K_3'(\Omega, E; T) + K_3'(\Omega, -E; T) \\ &+ K_3'(-\Omega, -E; T), \end{aligned} \quad (11)$$

with

$$\begin{aligned} K_3'(\Omega, E; T) &= \frac{8\pi}{\hbar} \frac{N(0)}{N} \alpha^2 (|\Omega|) \rho(E) \rho(E - \Omega) \frac{\Delta^2}{E(E - \Omega)} \\ &\times [f(\Omega - E) + n(\Omega)] \theta(\Omega - \Delta - E). \end{aligned} \quad (11a)$$

Now, we replace the steady-state energy gap in Eqs. (8)–(11) by the equilibrium gap $\Delta(T)$. Since all the terms in Eq. (8) are already of first order in the external disturbances, the correction is of higher order. The quasiparticle and phonon lifetimes τ_{qp} and τ_{ph} are given by

$$\tau_{qp}^{-1}(E, T) = \tau_s^{-1}(E, T) + \tau_R^{-1}(E, T) \quad (12)$$

and

$$\tau_{ph}^{-1}(\Omega, T) = \tau_{phs}^{-1}(\Omega, T) + \tau_B^{-1}(\Omega, T) + \tau_{os}^{-1}. \quad (13)$$

Here τ_s and τ_R are, respectively, the scattering and recombination lifetimes for quasiparticles in an equilibrium superconductor and τ_{phs} and τ_B are, respectively, the scattering and pair-breaking lifetimes for the phonons. These characteristic lifetimes have been studied in detail in Ref. 33, and various plots of their energy and temperature dependences are given there.

Since the RT equations have been applied in their linearized form to the study of quasiparticle recombination time, we discuss them in Appendix B in terms of the linearized coupled equations [Eqs. (8a) and (8b)].

Within the linear approximation, the change in the energy gap $\delta \Delta \equiv \Delta - \Delta(T)$ can be derived from Eq. (5). We have

equilibrium film under (a) thermal phonon injection, (b) microwave irradiation, (c) quasiparticle injection through a tunnel junction, and (d) optical irradiation.

In the first three cases only low-energy quasiparticle and phonon states are disturbed, while in case (d) electrons are excited into high-energy states. We consider cases (a)–(c) first and discuss case (d) last.

For cases (a)–(c) we replace the upper limits

of the integrals in Eq. (8) by a cutoff energy, 5Δ ; i.e., we ignore the deviation from equilibrium in the quasiparticle and phonon states with energy higher than the cutoff energy. This cutoff energy can be easily modified in our computer program. The results shown later have been checked and found to be unchanged by using a higher cutoff energy. 15 uniform mesh points are assigned for each energy interval of Δ for both quasiparticles and phonons. However, because the kernel K_i consists of the quasiparticle density of states which diverges at the gap edge, one cannot interpolate directly to write the integrals as summations. What we did is to do interpolations for the distributions $\delta f(E)$ and $\delta n(\Omega)$ only. The coefficients of $\delta f(E_i)$ and $\delta n(\Omega_j)$ which arise from the integration of the kernels can then be calculated using simple transformations to eliminate the divergence in K_i . When this is done, Eqs. (8a) and (8b) can be combined in the simple matrix form

$$\sum_j M_{ij} x_j = I_i, \quad (15)$$

with $1 \leq i, j \leq 136$ and

$$x_j = \begin{cases} \delta f(E_j) & \text{if } j \leq 61, \\ \delta n(\Omega_j) & \text{if } j > 61, \end{cases} \quad (16)$$

$$I_i = \begin{cases} I_{qp}(E_i) & \text{if } i \leq 61, \\ I_{ph}(\Omega_i) & \text{if } i > 61, \end{cases} \quad (17)$$

where $E_j = \Delta + \frac{1}{15}(j-1)\Delta$ and $\Omega_j = \frac{1}{15}(j-61)\Delta$. The vector \vec{x} can then be obtained by inverting the matrix \underline{M} when the driving term \vec{I} is given.

A. Thermal phonon injection (heat pumping)

For the case of a thin film attached to a heater, the driving terms are

$$I_{qp}^a(E) = 0 \quad (18a)$$

and

$$I_{ph}^a(\Omega) = A[n(\Omega, T_H) - n(\Omega, T)], \quad (18b)$$

where T and T_H are, respectively, the ambient temperature and the heater temperature. The coefficient A has been studied by Little⁴⁵ and found to be dependent upon the acoustic match and the temperature difference between the heater and the sample as well as the frequency of the phonon transmitted. Here we will treat A as a constant parameter in our problem. By using the equilibrium phonon distributions in Eq. (18) we have neglected, in $I_{ph}^a(\Omega)$, terms of order $A\delta n(\Omega)$ which are of second order in A .

As a typical experimental situation we set $T = \frac{1}{2}T_c$ so that the equilibrium gap is well formed and take $T_H = \frac{4}{3}T_c$. The steady-state phonon spec-

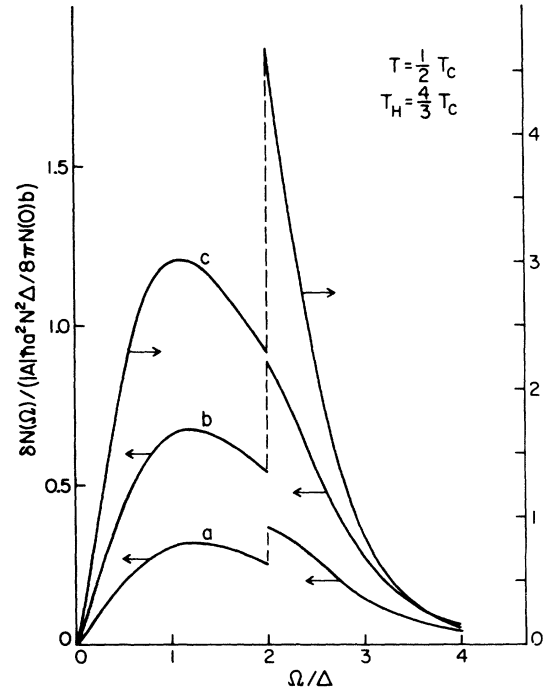


FIG. 2. Excess phonon spectra in a superconducting thin film pumped by a heater. Curves (a), (b), and (c) correspond to phonon escape times equal to $\tau_B(2\Delta)$, $2\tau_B(2\Delta)$, and $8\tau_B(2\Delta)$, respectively.

tra of the excess phonons in the nonequilibrium thin film are shown in Fig. 2 for phonon escape times $\tau_{es} = \tau_B(2\Delta, T)$, $2\tau_B(2\Delta, T)$, and $8\tau_B(2\Delta, T)$, respectively. Here $\tau_B(2\Delta, T)$ is the pair-breaking lifetime of phonons with energy $\hbar\Omega = 2\Delta$ in an equilibrium superconductor. In discussing the nonequilibrium phonons since $n(\Omega)$ diverges as $\Omega \rightarrow 0$ it is more physical to multiply $\delta n(\Omega)$ by the phonon density of states $NF(\Omega)$ giving $\delta N(\Omega) = \delta n(\Omega)NF(\Omega)$, which we have called the excess phonon spectra. First notice that, although the phonon injection rate is a smooth function, the spectra show a discontinuity at a phonon energy $\hbar\Omega = 2\Delta$. This is because high-energy phonons break pairs and create quasiparticles which are then scattered into low-energy states with the emission of phonons. The quasiparticle density of states has an inverse-square-root divergence at $E = \Delta$ and vanishes for $E < \Delta$. Thus, when these low-energy quasiparticles recombine, a sharp discontinuity in the phonon spectra at $\hbar\Omega = 2\Delta$ results. Secondly, when the phonon escape time is long, more phonons are trapped inside the sample. This occurs for phonons of energy smaller than 2Δ as well as greater than 2Δ . Thirdly, the spectral width of phonons with $\hbar\Omega \sim 2\Delta$ becomes sharper as the phonon escape time τ_{es} is increased. This can be understood by realizing that

a large τ_{es} means phonons of energy $\hbar\Omega \geq 2\Delta$ are more likely to break pairs than to escape from the superconducting film. Therefore, the energy originally carried by a phonon with $\hbar\Omega \geq 2\Delta$ has to be transferred to the quasiparticles more times before it is released from the thin film. Thus the quasiparticles created by the phonon pair breaking have more chance to be scattered to low-energy states and emit phonons of $\hbar\Omega \sim 2\Delta$ when they combine into pairs. We have also found that when the heater temperature increases the jump in the phonon spectra at $\hbar\Omega = 2\Delta$ becomes more dramatic because more high-energy phonons are available to be converted into phonons of energy $\hbar\Omega \sim 2\Delta$.

The phonon emission spectrum of the nonequilibrium film is $\delta N(\Omega)/\tau_{es}$ in our model. It has the same energy dependence as $\delta N(\Omega)$ since τ_{es} is a constant. Our results agree qualitatively with those of Dayem and Wiegand,¹² but differ from that of Dynes and Narayanamurti¹⁹ who obtained phonon spectra peaked at states of energy slightly below $\hbar\Omega = 2\Delta$ and sharply cut off above it. The corresponding quasiparticle distributions are shown in Fig. 3. As the phonon escape time increases so that more phonons are trapped inside the film, the quasiparticle density increases. One would also expect that the discontinuity in the phonon spectrum at energy $\hbar\Omega = 2\Delta$ will lead to a discontinuity in the derivative of the quasiparticle distribution at $E = 3\Delta$ due to the phonon absorption by the quasiparticle of energy $E = \Delta$. However, since the quasiparticle distribution function at $E = 3\Delta$ is very small itself, the additional structure occurring there is not significant in our linear approximation.

As for the energy gap in the steady state, since $\delta f(E) > 0$ for all states, the gap is reduced in the driven state. We do not calculate the amount of reduction except to mention that in the linear ap-

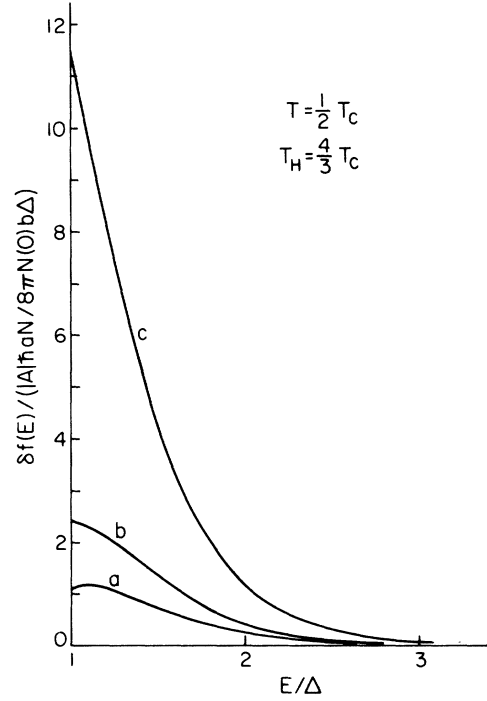


FIG. 3. Excess quasiparticle distributions corresponding to the phonon spectra shown in Fig. 2.

proximation it is proportional to the strength of the driving force.

B. Microwave irradiation

We consider a superconducting thin film irradiated by microwaves of frequency $\omega_0 = 0.5\Delta/\hbar$. Since the microwave photons have energy smaller than twice the energy gap, they cannot break pairs to create excess quasiparticles, but can excite quasiparticles from low-energy states into higher-energy states. The driving terms in this case are^{27,46}

$$I_{qp}^b(E) = \frac{B}{4N(0)\Delta} \frac{E - \omega_0}{[(E - \omega_0)^2 - \Delta^2]^{1/2}} \left(1 + \frac{\Delta^2}{E(E - \omega_0)}\right) [f(E - \omega_0, T) - f(E, T)] \theta(E - \omega_0 - \Delta) \\ + \frac{B}{4N(0)\Delta} \frac{E + \omega_0}{[(E + \omega_0)^2 - \Delta^2]^{1/2}} \left(1 + \frac{\Delta^2}{E(E + \omega_0)}\right) [f(E + \omega_0, T) - f(E, T)], \quad (19a)$$

$$I_{ph}^b(\Omega) = 0. \quad (19b)$$

In the following analysis we have smeared out the singularity in the driving term arising from gap edge by multiplying Eq. (19a) by $(\sqrt{\pi}\delta\omega)^{-1} \times \exp[-(\omega - \omega_0)^2/(\delta\omega)^2]$ and integrating over ω . Physically this represents a simple approximate way of taking into account the effects of the inhomogeneity and anisotropy of the gap parameter as well as lifetime broadening effects on the quasiparticle density of states near the gap edge. With $\delta\omega$ set to

be 0.1Δ and the temperature $T = 0.5T_c$, we calculated the steady-state excess distributions of quasiparticles and phonons. In order to get some insight into the effect on the distributions of the various pieces in the kinetic equations we will begin by discussing results obtained when only certain terms are kept. First consider the simplest "lifetime approximation" in which only the first two terms on the right-hand side of Eq. (8a)

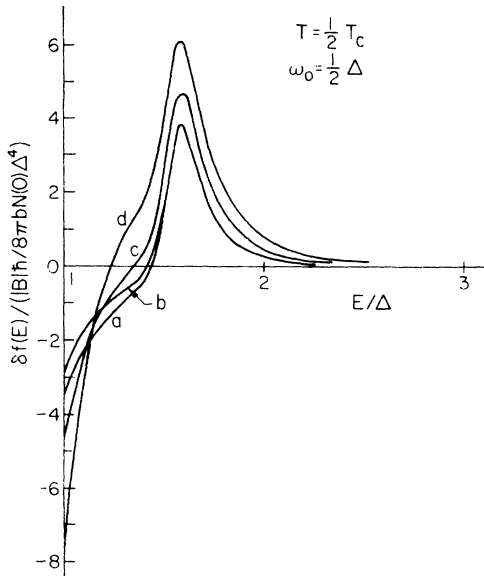


FIG. 4. Excess quasiparticle distributions in a superconducting thin film irradiated by microwaves. Curve (a) is obtained from the lifetime approximation. Curves (b), (c), and (d) are solutions of the linearized kinetic equations with $\tau_{es} = 0$, $\tau_B(2\Delta)$, and $8\tau_B(2\Delta)$, respectively.

are kept and the phonons are assumed to be in thermal equilibrium. The numerical solution of $\delta f(E)$ using this lifetime approximation is shown as curve (a) in Fig. 4. Curve (b) shows $\delta f(E)$ when the quasiparticles are treated exactly in the linear approximation, and the phonons are again assumed to be in equilibrium at an ambient temperature T . The solutions of $\delta f(E)$ for the full linearized kinetic equations, Eqs. (8a) and (8b), are shown as curves (c) and (d) with the phonon escape times $\tau_{es} = \tau_B(2\Delta, T)$ and $8\tau_B(2\Delta, T)$, respectively. [We note that curve (b) represents the solution of the linearized coupled kinetic equations with $\tau_{es} = 0$.] The general feature of these curves is a negative excess distribution for low-energy states with $E \sim \Delta$ and a positive excess distribution for states of $E \sim \Delta + \hbar\omega_0$. This reflects the fact that in an equilibrium superconductor most quasiparticles are distributed in states of $E \sim \Delta$ due to the inverse square root singularity in the density of states at $E = \Delta$. When the film is irradiated by microwaves, some of the quasiparticles in states $E \approx \Delta$ are excited to states with energy $E \approx \Delta + \hbar\omega_0$. In fact, if we had not smoothed out the singularity in the driving term of $I_{qp}^b(E)$ [Eq. (19a)], $\delta f(E)$ would diverge at $E = \hbar\omega_0 + \Delta$ reflecting the singularity in the density of states at the gap edge. The energy spectra of the excess phonons are shown in Fig. 5. For the cases (a) and (b) of Fig. 4, in which the phonons are assumed to be in equilibrium at the ambient temperature, the excess pho-

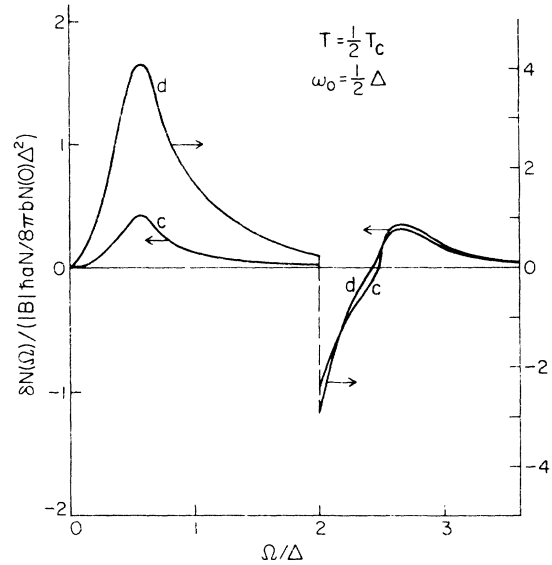


FIG. 5. Excess phonon spectra corresponding to the excess quasiparticle distributions shown as curves (c) and (d) in Fig. 4.

non distributions vanish. Curves (c) and (d) of Fig. 5 are the excess phonon energy distributions with $\tau_{es} = \tau_B(2\Delta, T)$ and $8\tau_B(2\Delta, T)$, respectively. The peaks in these distributions at $\hbar\Omega \sim \hbar\omega_0$ are due to phonons emitted by the excited quasiparticles when they relax back to the gap edge. When the phonon escape time increases, the peak height increases, because more emitted phonons are trapped in the film. The dip in the phonon spectra at a phonon energy $\hbar\Omega \sim 2\Delta$ is due to the fact that in the nonequilibrium state there are fewer quasiparticles in the low-energy states near the gap edge than in equilibrium. Therefore phonons with energies $\hbar\Omega = 2\Delta$ or slightly higher break pairs trying to make up the deficiency in these quasiparticle states. When the phonon escape time is larger, it is more difficult for the phonons of these energies to cross the boundary and get into the thin film. This leads to a more severe deficit in the phonons of these energies. The weak peaks in the phonon spectra at energies $\hbar\Omega \approx 2\Delta + \hbar\omega_0$ are due to phonon emission by the excess quasiparticles of energy $E \sim \Delta + \hbar\omega_0$ when they combine into pairs with quasiparticles near the gap edge.

As mentioned in the Introduction, experimentally it has been found that the critical current of a superconducting microbridge can be increased by microwave irradiation.^{16, 17} Eliashberg²⁷ suggested that this could be due to the fact that a low-energy quasiparticle is more effective in interfering with the pairing processes than quasiparticles of higher energies. Since microwave photons excite quasiparticles from low-energy states to high-energy

states, the pairing processes are interfered with to a lesser extent. This results in a larger gap and hence increases the critical current. In his investigation, a constant decay time was assumed. With microwave photons being unable to break pairs, this assumption leads to a total quasiparticle density equal to that in equilibrium. However, as discussed in Appendix B, the decay rate of the excess quasiparticle density depends upon the average of the inverse recombination time of the excess quasiparticles and the average of the inverse pair-breaking time of the excess phonons. Therefore, with the energy dependence of the decay times taken into account, the quasiparticle density in general should differ from the equilibrium value even when the film is irradiated by microwaves of frequency $\omega_0 < 2\Delta/\hbar$. In fact, the quasiparticle density for the driven state can be smaller than that in the equilibrium state. This decrease in the density of quasiparticles will also lead to an increase in the gap. The decrease in the quasiparticle density is due to the fact that the microwave photons excite quasiparticles into higher-energy states which have shorter recombination lifetimes compared to the low-energy states. When the phonon escape time increases, the phonon-trapping effect becomes important, and the total quasiparticle density increases as demonstrated in case (A). For the extreme case of $\tau_{\text{es}} = \infty$, phonons cannot escape from the film at all. Therefore, there is no energy outlet, and the film will be "heated up" by the microwaves. Eventually the film will be driven into the normal state.

C. Electron injection

We consider a superconducting thin film which forms part of a normal-insulator-superconductor tunnel junction. With a bias voltage, the tunnel current injects quasiparticles into the superconducting thin film. The driving terms in this case are²

$$I_{\text{qp}}^c(E) = \frac{C}{4N(0)\Delta} [f(E - eV, T) - f(E + eV, T)]\theta(E - \Delta), \quad (20a)$$

$$I_{\text{ph}}^c(\Omega) = 0, \quad (20b)$$

where the constant coefficient C depends upon the coupling between the normal metal and the superconductor and is proportional to the conductivity of the junction when the superconductor is in the normal state. In general, superconductors driven by current injection have to be treated carefully with the quasiparticle branch imbalance^{15, 38} in mind. However, within the linearized regime as long as

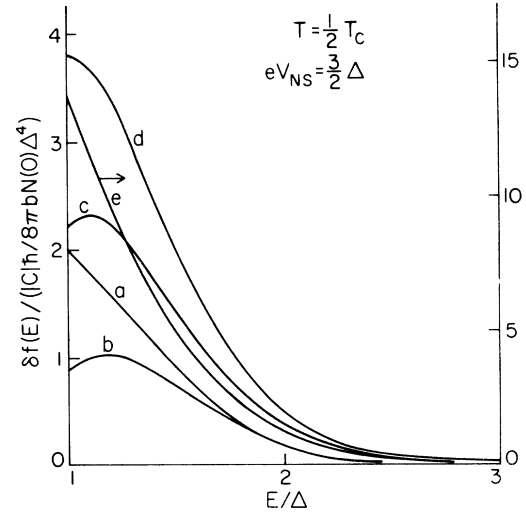


FIG. 6. Excess quasiparticle distributions in a superconducting thin film which is injected with quasiparticles from a NIS tunnel junction. See text for details.

the total quasiparticle distribution $\delta f(E) = \delta f_{>}(E) + \delta f_{<}(E)$ is concerned, the branch imbalance does not come into play. Here $\delta f_{>}(E)$ and $\delta f_{<}(E)$ are, respectively, the distribution functions for quasiparticles on the branch corresponding to the wave vector being greater than and smaller than the Fermi wave vector. We set the bias voltage $eV = 1.5\Delta$ and the temperature $T = 0.5T_c$. The solutions for the excess quasiparticle distribution are shown in Fig. 6. With the phonons assumed to be in equilibrium at temperature T (i.e., $\tau_{\text{es}} = 0$) curve (a) is the solution for $\delta f(E)$ within the decay-time approximation while curve (b) is the solution for the full linearized quasiparticle kinetic equation. The reason that curve (b) lies below curve (a) is that in the decay-time approximation each recombination event is considered to eliminate only one quasiparticle instead of two. Curves (c), (d), and (e) are solutions of $\delta f(E)$ keeping all the terms in Eqs. (8a) and (8b) with the phonon escape times $\tau_{\text{es}} = \tau_B(2\Delta, T)$, $2\tau_B(2\Delta, T)$, and $8\tau_B(2\Delta, T)$, respectively. As in the heat-pumping case, when the phonon escape time increases $\delta f(E)$ increases. We also note that in curves (b) and (c), a maximum in $\delta f(E)$ occurs at an energy slightly greater than Δ . This is because phonons can scatter quasiparticles in low-energy states to higher-energy states. When τ_{es} increases, more phonons of energy $\hbar\Omega \sim 2\Delta$ are trapped as shown in Fig. 7. They create quasiparticles of energy $E \sim \Delta$ when they break pairs and hence shift the maximum towards Δ . The excess phonon spectra are shown in Fig. 7. The spectrum corresponding to $\tau_{\text{es}} = 0$ vanishes and is not shown. Curves (c), (d), and (e) are the $\delta N(\Omega)$'s corresponding to curves (c), (d), and (e)

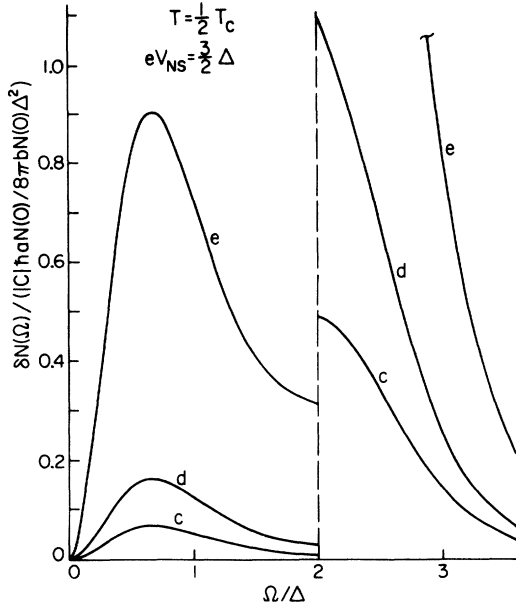


FIG. 7. Excess phonon spectra corresponding to the excess quasiparticle distributions shown as curves (c), (d), and (e) in Fig. 6.

for the $\delta f(E)$ in Fig. 6. Again, we note that the excess density increases for larger τ_{es} . However, the excess phonon density lies mainly at energies above 2Δ . This is because for $eV = 1.5\Delta$ most quasiparticles injected into the superconductor are near the gap edge. They are most likely to emit phonons of energy $2\Delta < \hbar\Omega < 3\Delta$ when they combine into pairs with quasiparticles near the gap edge. According to the calculation of Ref. 33, at $T = 0.5T_c$ quasiparticles with energy $E < 1.5\Delta$ are more likely to recombine into pairs than to be scattered into lower states, and hence few excess low-energy phonons are created. In view of the fact that few phonons of $\hbar\Omega < 2\Delta$ are emitted in the low-energy quasiparticle injection process, this may be a more favorable process for the generation of narrow band phonons of frequency $\omega = 2\Delta/\hbar$ than the heat-pulse-pumping process.

As for the change in the energy gap, as discussed in case (A), because the excess distribution function $\delta f(E)$ is positive for all quasiparticle states, the gap is reduced. Within the linear approximation we have employed, the change in the gap parameter is proportional to the strength of the driving force, and we will not calculate it.

D. Optical irradiation

Since optical photons have energy $\hbar\omega_L \gg 2\Delta$ they can break pairs as well as scatter quasiparticles. Therefore, one might be tempted to use Eq. (19) for the injection terms, with the addition of a

third term in Eq. (19a) to account for the pair-breaking processes of the photons.²⁹ However, this would require a dynamic treatment over a wide range of excitation energies. Furthermore, at these higher energies electron-electron interactions must be included. Now we know that, due to the short lifetimes associated with the high-energy excitations, the steady-state quasiparticle and phonon distributions differ from their respective equilibrium values only for energies up to a few times the gap energy. Therefore it is sufficient to introduce a pseudoinjection term which describes the resultant injection over a low-frequency region due to the decay of quasiparticles and phonons with higher energies. As discussed below, these pseudoinjection terms have a simple form. For real systems in which τ_{es} is nonvanishing, the pseudoinjection is dominated by phonons so that

$$I_{qp}^d(E) = 0 \quad (21a)$$

and

$$I_{ph}^d(\Omega) = D. \quad (21b)$$

Here D is an energy-independent constant which varies with the frequency as well as the intensity of the optical radiation.

In order to understand the details of the decay processes in a superconductor with high energy excitations which lead to Eqs. (21a) and (21b), we first note that in a normal metal, the inverse of the electron lifetime of energy E is given by⁴⁷

$$\tau_{el}^{-1}(E) = 2\omega_D \left(0.252 r_s^{1/2} \frac{\omega_D}{E_f} \left(\frac{E}{\omega_D} \right)^2 + 0.174 r_s \left\{ \left(\frac{E}{\omega_D} \right)^3, 1 \right\}_{\min} \right). \quad (22)$$

Here E is measured from the chemical potential (E_f) of the metal. The first term is contributed by the electron-electron interactions while the second term arises from the electron-phonon interactions. The curly bracket $\{\cdot\cdot\}_{\min}$ represents the smaller value in the parentheses, while r_s is defined as usual so that $\frac{4}{3}\pi(r_s a_0)^3$ is equal to the inverse of the electron density with a_0 being the Bohr radius. For real solids $6 > r_s > 2$. Therefore, there is a characteristic energy $\hbar\bar{\omega} \approx (E_f \omega_D)^{1/2}$ such that the lifetimes of quasiparticles of energy greater than $\hbar\bar{\omega}$ is dominated by electron-electron interactions instead of electron-phonon interactions. The characteristic energies for Al, Sn, and Pb are given in Table I with the wavelength of the optical radiation assumed to be $\lambda = 5000 \text{ \AA}$. Also given in Table I are the Fermi energy E_f , the Debye energy $\hbar\omega_D$ and r_s for these materials.⁴⁸

TABLE I. Characteristic energy $\hbar\bar{\omega}$, Fermi energy E_f , Debye energy $\hbar\omega_D$ and γ_s for Al, Sn, and Pb.

	r_s^a	$\hbar\omega_D$ (°K) ^a	E_f (eV) ^a	$\hbar\bar{\omega}/\hbar\omega_D$	$\hbar\omega_L/\hbar\omega_D^b$
Al	2.07	428	11.63	17.64	67.20
Sn	2.23	200	10.03	24.87	143.80
Pb	2.30	105	9.37	33.70	273.91

^a Data are quoted from C. Kittel, *Introduction to Solid State Physics*, 4th ed. (Wiley, New York, 1971).

^b The optical photon energy $\hbar\omega_L$, which corresponds to wavelength $\lambda = 5000 \text{ \AA}$, is 2.48 eV.

With the data given in Table I, it is possible to draw the following picture about what happens in a superconductor irradiated by light. An electron of energy $E > \hbar\bar{\omega}$ excited by an optical photon first loses energy to other electrons via electron-electron

interactions. After one or two collisions, its energy falls below $\hbar\bar{\omega}$, and it decays by emitting phonons. On the average, more than 15 phonons will be emitted before the electron drops into states of energy smaller than the Debye energy.

The emitted phonons can either break pairs to create quasiparticles or escape from the sample. Since the phonon trapping effect is already important in experiments in which only low-energy excitations are created, this effect will be more severe for the high-energy phonons involved in this case. Thus, phonons create many more quasiparticles than those generated directly by the optical photons and by the electron-electron interactions. We therefore neglect the direct contribution to the quasiparticle driving term due to the electron-photon interactions and electron-electron interactions and have Eq. (21a).

The phonon generation rate due to the decay of electrons with energy $\hbar\bar{\omega} > E > \hbar\omega_D$ is proportional to

$$I_{\text{ph}}^d(\Omega) \propto \int_{\hbar\omega_D}^{\hbar\bar{\omega}} dE \int_{\hbar\omega_D}^{\hbar\bar{\omega}} dE' \alpha^2(\Omega) \{f(E)[1-f(E')][n(\Omega)+1] - f(E')[1-f(E)]n(\Omega)\} \delta(E'+\Omega-E). \quad (23)$$

Since $\bar{\omega}_L \gg \omega_D$, $\rho(E) \approx 1$, and $\delta f(E)$ and $\delta n(\Omega)$ are much smaller than unity in the interested energy region, this can be simplified to give

$$I_{\text{ph}}^d(\Omega) \propto \int_{\hbar\omega_D}^{\hbar\omega_L} dE \alpha^2(\Omega) \delta f(E).$$

This expression leads to the phonon injection term given by Eq. (21b) when the energy dependence of $\alpha^2(\Omega)$ is neglected.

When the computer program is actually run, we use cutoff energies of 5Δ , 7Δ , and 9Δ for both the quasiparticle and phonon states. We found that although the shapes of the distribution functions differ slightly for cutoff energies equal to 5Δ and 7Δ , there is essentially no difference between those using cutoff energies 7Δ and 9Δ . This result indicates that a cutoff energy of 9Δ is sufficient to obtain the steady-state distributions. We also conclude from this result that the detailed structures of the phonon density of states and $\alpha^2(\Omega)$ in the region of energy greater than 9Δ are not important. Instead, it is the phonon escape time which is most important in the determination of the laser-driven steady state.

In Fig. 8 we show the excess quasiparticle distributions. The excess phonon spectra are shown in Fig. 9. Curves (a) and (b) correspond to phonon escape times $\tau_{\text{es}} = 2\tau_B(2\Delta)$ and $8\tau_B(2\Delta)$, respective-

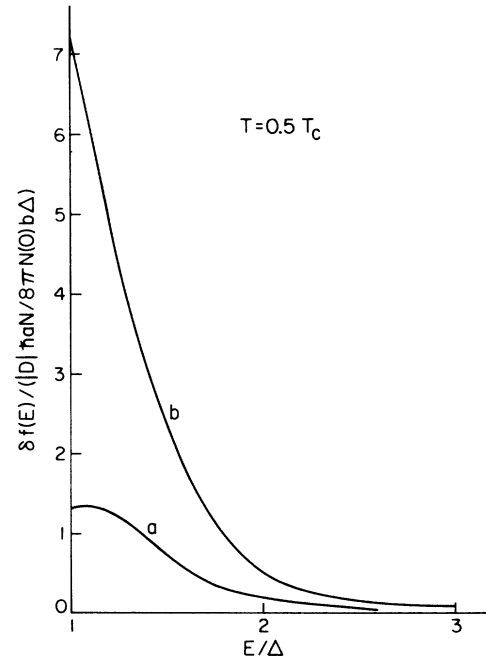


FIG. 8. Excess quasiparticle distributions in a superconducting thin film irradiated by light. Curves (a) and (b) correspond to the phonon escape times $\tau_{\text{es}} = 2\tau_B(2\Delta)$ and $8\tau_B(2\Delta)$, respectively.

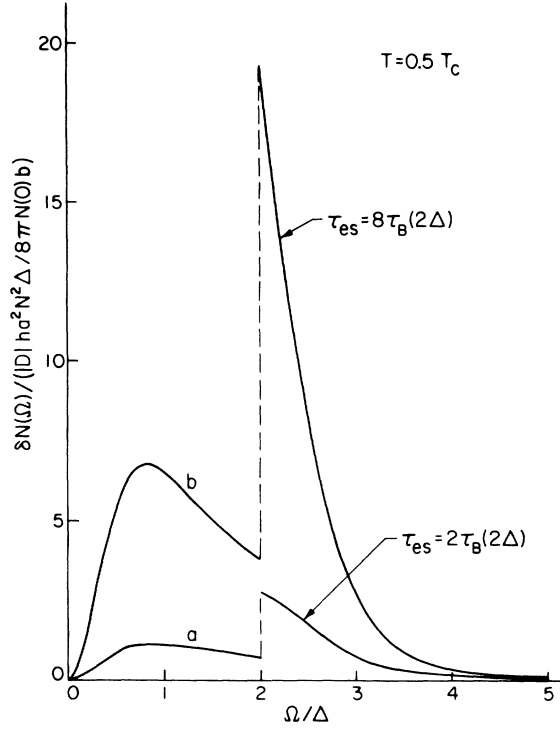


FIG. 9. Excess phonon spectra corresponding to the excess quasiparticle distribution shown in Fig. 8.

ly. The sharp structure in the excess phonon spectra near $\hbar\Omega = 2\Delta$ indicates that the steady state cannot be described by the simple heating theory. On the other hand, if the spectrum were only observed in the energy region $\hbar\Omega < 2\Delta$, it would appear similar to a heating effect.

IV. TRANSPORT PROPERTIES

In this section we study (a) the ultrasonic attenuation coefficient, (b) the electric conductivity for a superconductor in the driven states, and (c) the $I(V)$ characteristic of an SIS tunnel junction with a nonequilibrium superconducting thin film forming part of the junction. We calculate the deviation of these transport properties from their equilibrium values using the excess quasiparticle distributions obtained in Sec. III. We do not consider the transport properties of thin films irradiated by light. Judging from the similarity in the quasiparticle distributions resulted from optical radiations and thermal phonon injections they will be similar to those of films pumped by heat.

A. Ultrasonic attenuation coefficient

The ultrasonic attenuation coefficient of a thin film in the equilibrium superconducting state when normalized by its normal state value is given by⁴⁹

$$\frac{\alpha_s(\Omega, \Delta(T), T)}{\alpha_N(\Omega)} = \frac{2}{\Omega} \left(\int_{\Delta(T)}^{\infty} dE \frac{E(E+\Omega) - \Delta^2(T)}{\{[E^2 - \Delta^2(T)][(E+\Omega)^2 - \Delta^2(T)]\}^{1/2}} [f(E, T) - f(\Omega+E, T)] \right. \\ \left. + \frac{1}{2} \int_{\Delta(T)}^{\infty} dE \theta(\Omega - 2\Delta(T)) \frac{E(\Omega - E) + \Delta^2(T)}{\{[E^2 - \Delta^2(T)][(\Omega - E)^2 - \Delta^2(T)]\}^{1/2}} [1 - f(E, T) - f(\Omega - E, T)] \right). \quad (24)$$

Here $\alpha_s(\Omega, \Delta(T), T)$ and $\alpha_N(\Omega, T)$ are, respectively, the temperature-dependent superconducting state and normal state phonon attenuation coefficients for a phonon of energy $\hbar\Omega$. The steady-state attenuation coefficient of a superconductor in the driven state is denoted by $\alpha_s(\Omega, \Delta)$ with Δ being the steady-state energy gap. To calculate $\alpha_s(\Omega, \Delta)/\alpha_N(\Omega, T)$, we replace the gap $\Delta(T)$ by Δ and the Fermi function $f(E', T)$ by the steady-state quasiparticle distribution function $f(E')$ in Eq. (24).

It is convenient to define an excess attenuation coefficient

$$\delta\alpha_s(\Omega, \Delta) \equiv \alpha_s(\Omega, \Delta) - \alpha_s(\Omega; \Delta, T). \quad (25)$$

We note that $\delta\alpha_s(\Omega, \Delta)$ is not the difference between the steady-state attenuation coefficient $\alpha_s(\Omega, \Delta)$ and that in the equilibrium state $\alpha_s(\Omega, \Delta(T), T)$ because in the second term in Eq. (25) we have used the steady-state energy gap instead of the equilibrium gap $\Delta(T)$. In fact, they differ by an amount of $[\alpha_s(\Omega, \Delta, T) - \alpha_s(\Omega, \Delta(T), T)]$ which can be calculated using Eq. (24) if the steady state gap Δ is determined.

From Eqs. (7a), (24) and (25) we have for $\delta\alpha_s(\Omega, \Delta)$

$$\frac{\delta\alpha_s(\Omega, \Delta)}{\alpha_N(\Omega, T)} = \frac{2}{\Omega} \left(\int_{\Delta}^{\infty} dE \frac{(E+\Omega)E - \Delta^2}{\{[E^2 - \Delta^2][(E+\Omega)^2 - \Delta^2]\}^{1/2}} \delta f(E) - \int_{\Delta+\Omega}^{\infty} dE \frac{E(E-\Omega) - \Delta^2}{\{[E^2 - \Delta^2][(E-\Omega)^2 - \Delta^2]\}^{1/2}} \delta f(E) \right. \\ \left. + \int_{\Delta}^{\Omega-\Delta} dE \theta(\Omega - 2\Delta) \frac{E(\Omega - E) + \Delta^2}{\{[E^2 - \Delta^2][(\Omega - E)^2]\}^{1/2}} \delta f(E) \right). \quad (26)$$

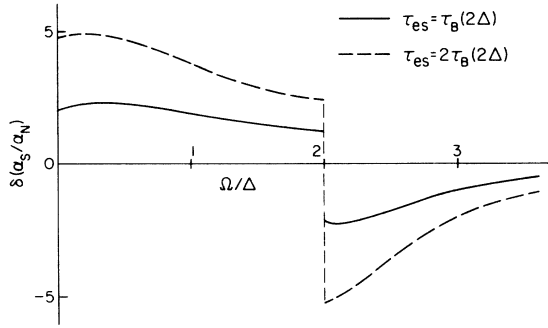


FIG. 10. Frequency dependence of $\delta(\alpha_s/\alpha_N)$ for a superconducting thin film pumped by a heater. The heater temperature and ambient temperatures are, respectively, $\frac{4}{3}T_c$ and $\frac{1}{2}T_c$.

Thus the excess ultrasonic attenuation coefficient is related to the excess quasiparticle distribution by a linear integral equation. We would like to emphasize here that to obtain Eq. (26) we did not use the linear approximation. The linear relation between $\delta\alpha_s$ and $\delta f(E)$ is a result of the Fermi golden-rule approximation. However, in the following, the $\delta\alpha_s(\Omega, \Delta)$ presented are calculated from $\delta f(E)$ obtained from the linearized coupled kinetic equations.

Figure 10 shows the excess ultrasonic attenuation coefficient $\delta\alpha_s(\Omega, \Delta)/\alpha_N(\Omega, T)$ for a superconductor attached to a heater. The solid and dashed curves are, respectively, obtained from the excess quasiparticle distributions shown in curves (a) and (b) of Fig. 3. They correspond to phonon escape times $\tau_{es} = \tau_B(2\Delta)$ and $2\tau_B(2\Delta)$ respectively. For phonons of energy $\hbar\Omega < 2\Delta$, only scattering processes contribute to the attenuation. The presence of the excess quasiparticles increase the electron-phonon scattering cross sections and results in the increase of the phonon attenuation coefficient. However for phonons of energy $\hbar\Omega \geq 2\Delta$, the attenuation coefficient is reduced. This can be understood by realizing that these phonons decay mainly by breaking pairs. With excess quasiparticles present, more quasiparticle states are blocked due to the Pauli exclusion principle, therefore pair breaking processes are less likely to occur than in the equilibrium case. When the suppression of the attenuation coefficient due to the blocking of the pair-breaking processes overcomes the enhancement due to the scattering processes, the excess quasiparticles give a net reduction of $\alpha_s(\Omega, \Delta)$.

The situation for the case of microwave irradiation is slightly complicated. In Fig. 11 we plot the excess attenuation coefficients calculated from the $\delta f(E)$'s shown in Fig. 4 as curves (b) and (d). The solid and the dashed curves correspond, respec-

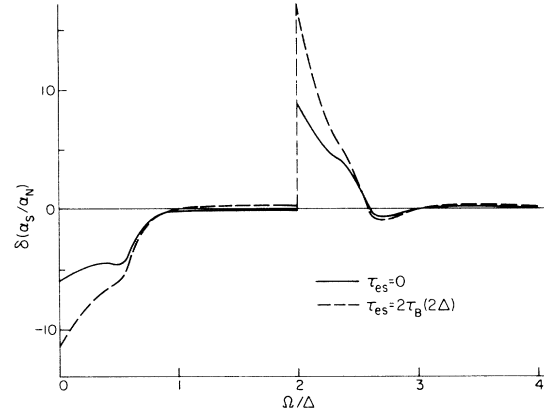


FIG. 11. Frequency dependence of $\delta(\alpha_s/\alpha_N)$ for a superconducting thin film irradiated by microwaves of frequency $\omega_0 = 0.5 \Delta/\hbar$. The ambient temperature is $\frac{1}{2}T_c$.

tively, to phonon escape times $\tau_{es} = 0$ and $2\tau_B(2\Delta, T)$. We consider first the attenuation of low-frequency phonons of energy $\hbar\Omega \sim 0$. The attenuation coefficient for these phonons is suppressed. This can be understood by observing the fact that a low-energy quasiparticle is more effective in the scattering of phonons than quasiparticles of higher energy. We note first that a low-energy quasiparticle when scattered by a phonon goes into states with energy lower than that resulting from the scattering of a higher-energy quasiparticle by the same phonon. Since the density of quasiparticle states increases at lower energy, the electron-phonon scattering cross section for a low-energy quasiparticle is larger than that of higher-energy quasiparticles due to the larger final density of states involved. Since microwave photons excite quasiparticles from low-energy states into higher-energy states, a reduction in the attenuation coefficient results.

For the attenuation of phonons of higher energy, the difference in the final quasiparticle density of states associated with the scattering processes becomes less significant. Instead, the attenuation coefficient contributed by the scattering processes [the first two terms of Eq. (26)] approaches $2\delta N_{qv}/\Omega$ when $\Omega \gg \Delta$, so that only the total number of excess quasiparticles are important. Although due to the coherence factor, $\delta\alpha_s(\Omega, \Delta)/\alpha_N(\Omega, T)$ contributed by scattering has not quite yet converged to its asymptotic value at $\Omega \approx 2\Delta$, the small value of the excess attenuation coefficient indicates that the excess quasiparticle densities are small in these cases.

When the phonon energy exceeds 2Δ , pair-breaking sets in and it dominates the phonon attenuation. With the microwave exciting quasiparticles out of the low-lying states near the gap edge, there are

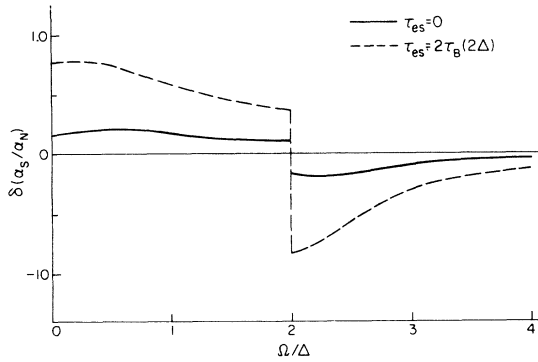


FIG. 12. Frequency dependence of $\delta(\alpha_s/\alpha_N)$ for a superconducting thin film under quasiparticle injection through a NIS tunnel junction. The bias voltage is $1.5\Delta/e$ with the ambient temperature fixed at $0.5T_c$.

more available final states for the quasiparticles which are produced in pair-breaking processes by phonons of energy equal to or slightly greater than 2Δ .

The excess attenuation coefficient for a thin film

$$\frac{\sigma_{1s}(\omega, T)}{\sigma_N} = \frac{2}{\omega} \left(\int_{\Delta(T)}^{\infty} dE \frac{E(E+\omega) + \Delta^2(T)}{\{[E^2 - \Delta^2(T)][(E+\omega)^2 - \Delta^2(T)]\}^{1/2}} [f(E, T) - f(E+\omega, T)] \right. \\ \left. + \int_{\Delta(T)}^{\omega - \Delta(T)} dE \frac{E(\omega - E) - \Delta^2(T)}{\{[E^2 - \Delta^2(T)][(\omega - E)^2 - \Delta^2(T)]\}^{1/2}} [1 - f(E, T) - f(\omega - E, T)] \right) \quad (28a)$$

and

$$\frac{\sigma_{2s}(\omega, T)}{\sigma_N} = \frac{1}{\omega} \int_{(-\Delta(T), \Delta(T)-\omega)_{\max}}^{\Delta(T)} dE \frac{E(E+\omega) + \Delta^2(T)}{\{[\Delta^2(T) - E^2][(E+\omega)^2 - \Delta^2(T)]\}^{1/2}} [1 - 2f(E+\omega, T)]. \quad (28b)$$

Although the imaginary part of the conductivity is less transparent, the real part, $\sigma_{1s}(\omega, T)/\sigma_N$, which is related to the microwave absorption rate of the superconductor is easy to understand. The first and second integrals in Eq. (28a) can be attributed, respectively, to the quasiparticle scattering and pair breaking by the microwave photons. In fact $\sigma_{1s}(\omega, T)/\sigma_N$ has the same form as the sound-wave attenuation coefficient given by Eq. (24) except for the signs of Δ^2 in the numerators of the integrands due to the different coherence factors involved.

Following the same procedure used in discussing the sound wave attenuation, we define an excess conductivity due to the nonequilibrium distribution and obtain

$$\frac{\delta\sigma_{1s}(\omega)}{\sigma_N} = \frac{2}{\omega} \left(\int_{\Delta}^{\infty} dE \frac{E(E+\omega) + \Delta^2}{\{[E^2 - \Delta^2][(E+\omega)^2 - \Delta^2]\}^{1/2}} [\delta f(E) - \delta f(E+\omega)] \right. \\ \left. - \int_{\Delta}^{\omega - \Delta} dE \frac{E(\omega - E) - \Delta^2}{\{[E^2 - \Delta^2][(\omega - E)^2 - \Delta^2]\}^{1/2}} [\delta f(E) + \delta f(\omega - E)] \right) \quad (29a)$$

and

$$\frac{\delta\sigma_{2s}(\omega)}{\sigma_N} = -\frac{2}{\omega} \int_{(-\Delta, \Delta-\omega)_{\max}}^{\Delta} dE \frac{E(E+\omega) + \Delta^2}{\{[\Delta^2 - E^2][(E+\omega)^2 - \Delta^2]\}^{1/2}} \delta f(E+\omega). \quad (29b)$$

In Fig. 13, we plot $\delta\sigma_{1s}/\sigma_N$ and $\delta\sigma_{2s}/\sigma_N$ for the film under thermal phonon injection. The solid and dashed curves again correspond to the phonon escape times $\tau_{es} = \tau_B(2\Delta)$ and $2\tau_B(2\Delta)$. A kink appears at $\omega = 2\Delta$ for all curves although the struc-

ture there is weak especially for $\delta\sigma_{2s}/\sigma_N$. This feature differs from that in the attenuation coefficient which shows a discontinuity at $\Omega = 2\Delta$, because of the different coherence factors involved. The magnitude of the excess conductivity can be

B. Electric conductivity

According to Mattis and Bardeen,⁵⁰ the complex conductivity of a superconductor in thermal equilibrium can be written as

$$\sigma_s(\omega, T)/\sigma_N = \sigma_{1s}(\omega, T)/\sigma_N - i\sigma_s(\omega, T)/\sigma_N, \quad (27)$$

with

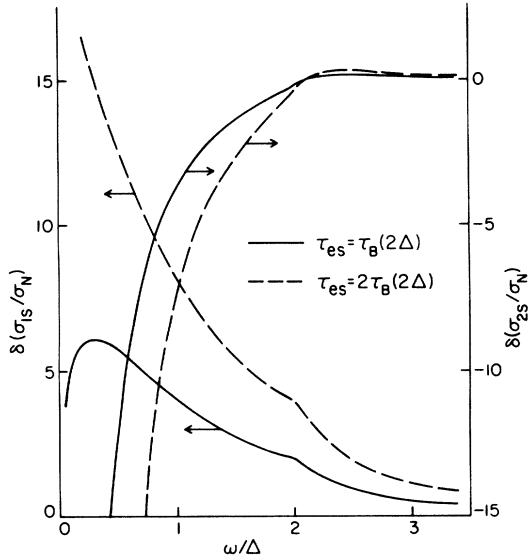


FIG. 13. Frequency dependences of $\delta(\sigma_{1s}/\sigma_N)$ and $\delta(\sigma_{2s}/\sigma_N)$ for a superconducting thin film pumped by a heater. The heater temperature and the ambient temperature are set at $\frac{4}{3}T_c$ and $\frac{1}{2}T_c$, respectively.

large at low frequencies, however the conductivity itself in this region is large and hence the deviation may not be easily observed. We also note that although for $\tau_{es}=0$, σ_{1s}/σ_N approaches $-\infty$ when the frequency $\omega \rightarrow 0$, it approaches $+\infty$ for $\tau_{es}=2\tau_B(2\Delta, T)$. This reflects the different signs of the first derivative of $\delta f(E)$ at the gap edge for the two different phonon escape times as shown in Fig. 3 [curves (a) and (b)]. It is easy to show that

$$\frac{\delta\sigma_{1s}(\omega)}{\sigma_N} \propto \frac{\partial\delta f(\Delta)}{\partial\Delta} \ln\omega \quad (30)$$

when $\omega \rightarrow 0$. Therefore a positive (negative) value of $\partial\delta f(\Delta)/\partial\Delta$ results in $\delta\sigma_{1s}(\omega) \rightarrow \infty(-\infty)$ when $\omega \rightarrow 0$. As discussed previously, gap inhomogeneity, anisotropy, and finite quasiparticle lifetime effects will cut off this low-frequency logarithmic divergence, and the structure there will be smeared out.

The excess conductivities for the film under microwave irradiation are shown in Fig. 14. The solid and dashed curves correspond to $\tau_{es}=0$ and $2\tau_B(2\Delta)$, respectively. The strong variation in the excess quasiparticle distributions of low-energy states leads to the complicated structures. In this case σ_{1s}/σ_N approaches $-\infty$ as expected to reflect the positive first derivative of $\delta f(E)$ at the gap edge.

In the electron-tunneling case, the excess conductivities of the films injected with quasiparticles are shown in Fig. 15. The phonon escape time is zero for the solid curve and $2\tau_B(2\Delta)$ for the dashed

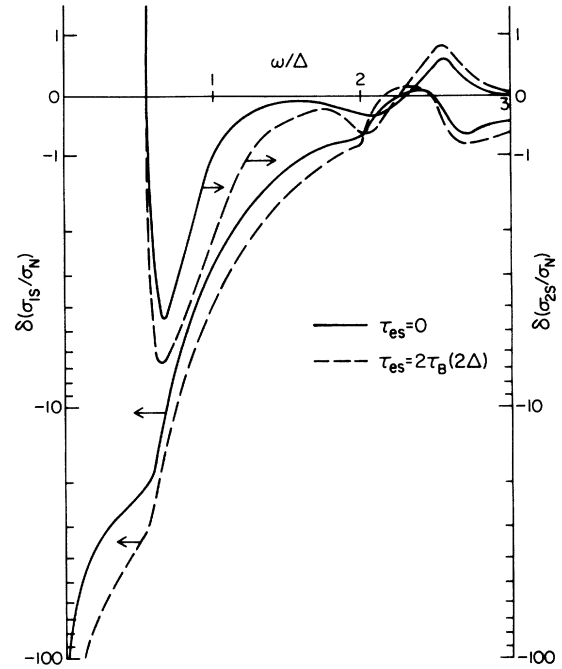


FIG. 14. Frequency dependences of $\delta(\sigma_{1s}/\sigma_N)$ and $\delta(\sigma_{2s}/\sigma_N)$ for a superconducting thin film irradiated by microwaves of frequency $\omega_0=0.5\Delta/\hbar$. The ambient temperature is $0.5T_c$.

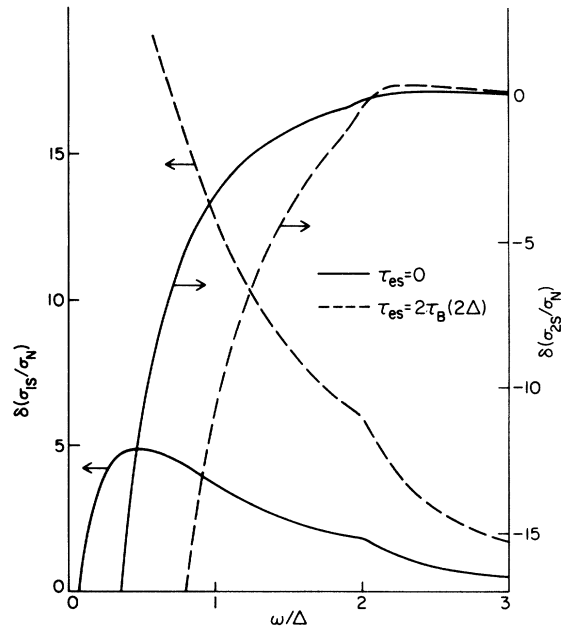


FIG. 15. Frequency dependences of $\delta(\sigma_{1s}/\sigma_N)$ and $\delta(\sigma_{2s}/\sigma_N)$ for a superconducting thin film under quasiparticle injection through a NIS tunnel junction. The bias voltage is $1.5\Delta/e$ with the ambient temperature fixed at $0.5T_c$.

curve. These curves resemble those in Fig. 13 and will not be discussed further.

C. $I(V)$ characteristics

We consider a superconductor-insulator-superconductor tunnel junction with the superconducting thin films on both sides of the junction made of the

$$\begin{aligned} \delta I(V) = & K \int_{\Delta}^{\infty} dE \frac{E(E+eV)\theta(E+eV-\Delta(T))}{\{(E^2-\Delta^2)[(E+eV)^2-\Delta^2(T)]\}^{1/2}} \delta f(E) - K \int_{\Delta}^{\infty} dE \frac{E(E-eV)\theta(E-eV-\Delta(T))}{\{(E^2-\Delta^2)[(E-eV)^2-\Delta^2(T)]\}^{1/2}} \delta f(E) \\ & - K \int_{\Delta}^{\infty} dE \frac{E(eV-E)\theta(eV-E-\Delta(T))}{\{(E^2-\Delta^2)[(eV-E)^2-\Delta^2(T)]\}^{1/2}} \delta f(E), \end{aligned} \quad (31)$$

where K is the normal state conductance divided by the magnitude of the electron charge. The energy gaps of the films in the driven state and the equilibrium state are denoted by Δ and $\Delta(T)$, respectively.

In Fig. 16 the solid curve shows the $I(V)$ characteristic of an SIS tunnel junction with one of the superconducting thin films pumped by a heater. For comparison, the $I(V)$ curve when both films are driven out of equilibrium to the same extent is shown as the dashed curve. The $\delta I(V)$ characteristics corresponding to the microwave-irradiation and electron-injection cases⁵¹ are shown in Figs. 17 and 18, respectively.

As discussed in the previous section, the gap parameter is depressed for thin films under heat pumping and quasiparticle tunneling injection and is enhanced for thin films under microwave irradiation (if the phonon escape time for the thin film is short enough). To obtain the results for the excess $I(V)$ characteristics we assumed that the gap is depressed by 5% from its equilibrium value for cases of heat pumping and quasiparticle tunneling injection and is enhanced by 5% for the case

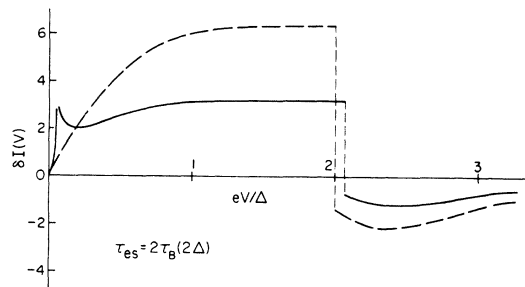


FIG. 16. Excess $I(V)$ characteristics of a nonequilibrium SIS tunnel junction. Solid curve: one of the superconducting film is driven out of equilibrium by thermal phonon injection. Dashed curve: both films are out of equilibrium to the same extent. The gap is assumed to be depressed by 5% from its equilibrium value.

same material. The $I(V)$ characteristics of such a junction with both films being driven out of equilibrium to the same extent have previously been discussed.³⁶ Here we study the situation in which only one of the superconducting films is in the driven state while the other film remains in equilibrium. In this case the excess tunnel current defined in Ref. 36 is given by

of microwave irradiation. We believe that at the ambient temperature $T = 0.5T_c$ this small change in the gap parameter is consistent with using the linearized kinetic equations.

We note first that a divergence in the tunneling current occurs at $eV = |\Delta(T) - \Delta|$ as found in an equilibrium tunnel junction made of superconducting thin films with different energy gaps. Secondly, except for near the voltage region where the tunneling current diverges; the magnitude of the tunneling current is about half that when both films are out of equilibrium. In fact it is easy to show that the value of the first integral in Eq. (31) approaches $K\Delta\delta N_{qp}$ while that of the second integral practically vanishes as $eV \gg \Delta$. Therefore the tunneling current contributed by the processes that give rise to the first two integrals in Eq. (31) has an asymptotic value of $K\Delta\delta N_{qp}$ at high voltages which differs by a factor of $\frac{1}{2}$ from the value of $2K\Delta\delta N_{qp}$ which was obtained for the case in which both films are in the driven state.³⁶

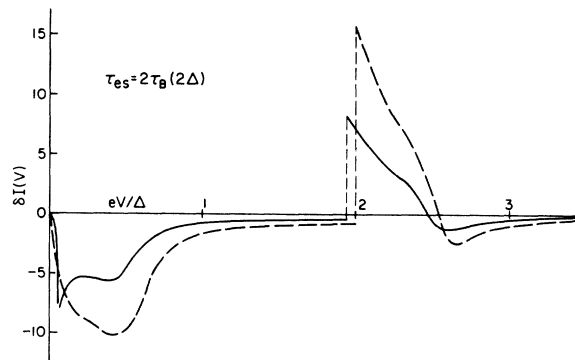


FIG. 17. Excess $I(V)$ characteristics of a nonequilibrium SIS tunnel junction. Solid curve: one of the superconducting thin films is driven out of equilibrium by microwave irradiation. Dashed curve: both films are out of equilibrium to the same extent. The gap is assumed to be enhanced by 5% from its equilibrium value.

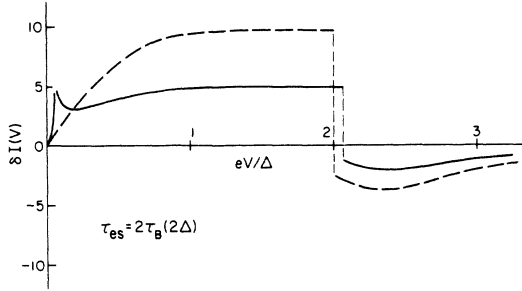


FIG. 18. Excess $I(V)$ characteristics of a nonequilibrium SIS tunnel junction. Solid curve: one of the superconducting thin films is driven out of equilibrium by quasiparticle tunneling. Dashed curve: both films are out of equilibrium to the same extent. The gap is assumed to be depressed by 5% from its equilibrium value.

V. CONCLUSION

Transport measurements should provide a direct probe of the quasiparticle and phonon distributions in the various nonequilibrium superconducting states. Because of the relative ease with which different energies can be probed by tunneling, it seems likely that the $I(V)$ characteristic will provide the most complete information on $f(E)$. It will be interesting to compare differences between $f(E)$ observed for a given gap reduction produced by the various external sources. Here we have sought to emphasize the characteristic signatures which appear in the transport coefficients when the system is driven into a nonequilibrium state by a particular external source.

In addition to these characteristics, two results seem particularly interesting to us. First, the kinetic equations provide detailed information on the structure of the phonon band generated near 2Δ . A superconductor driven by a heater converts high-frequency phonons into phonons of energy of order 2Δ . We found that the width of this phonon band near 2Δ depends upon the phonon escape time with the band narrower for longer phonon escape times. In addition, results for phonon generation due to quasiparticle tunnel injection were obtained which also showed a peaklike structure in the phonon distribution near 2Δ . This should be particularly interesting for the case in which the quasiparticles are injected across an SIS junction at a bias voltage close to $2\Delta/e$. Here we expect a large narrow band of 2Δ phonons to be generated. This configuration is investigated using the full set of nonlinear equations.⁵²

A second result of interest is the reduction of the density of quasiparticles for a superconducting film irradiated with microwaves having $\hbar\omega < 2\Delta$. The quasiparticle recombination rate increases with the quasiparticle energy since the phase space for phonon emission increases with the final state phonon energy. Thus quasiparticles excited from the gap edge Δ by the microwaves combine more rapidly than if they were left in equilibrium, resulting in a net decrease of quasiparticles in the driven state. The size of this effect depends upon the escape time for the emitted phonon to leave the sample. With a short escape time this process may allow a significant decrease in the quasiparticle density and provide an additional mechanism, beyond that proposed by Eliashberg,²⁷ for enhancing the gap.

Under a strong external drive the deviations of the quasiparticle and phonon distributions from their equilibrium values become large, and one must treat the full nonlinear equations. This is particularly true for monochromatic sources in which significant changes in the distributions can be produced in narrow ranges of energy. In this case the gap equation must be self-consistently solved along with the kinetic equations. In addition, the problems of transient response as well as inhomogeneous spatial excitation remain to be investigated. Finally, the nature of instabilities in the nonequilibrium state and the possibility of a driven mixed state represent open theoretical and experimental challenges.

APPENDIX A: ROTHWART-TAYLOR EQUATIONS

In this appendix we derive the RT equations from the coupled kinetic equations [Eq. (1)].

We define the quasiparticle density N_{qp} as

$$N_{qp} \equiv \int_{-\infty}^{+\infty} dE 2N(0)f(E), \quad (A1)$$

where $E = (\epsilon^2 + \Delta^2)^{1/2}$. $N(0)$ is the normal-state single-spin density of states at the Fermi surface. The factor of 2 takes into account the spin degree of freedom for the electrons. The phonon density for phonons of energy $\hbar\Omega \geq 2\Delta$, N_{ph} is given by

$$N_{ph} \equiv \int_{2\Delta}^{\infty} d\Omega NF(\Omega)n(\Omega). \quad (A2)$$

With these definitions Eq. (1a), after multiplying by $4N(0)\rho(E)$ and integrated over all quasiparticle states, gives

$$\frac{dN_{qp}}{dt} = I_{qp} - \frac{8\pi}{\hbar} N(0) \int_{\Delta}^{\infty} dE \int_{\Delta}^{\infty} dE' \alpha^2 F(E+E') \rho(E) \rho(E') \left(1 + \frac{\Delta^2}{EE'}\right) \times \{f(E)f(E')[n(E+E') + 1] - [1 - f(E)][1 - f(E')]n(E+E')\}, \quad (A3)$$

where

$$I_{qp} \equiv 4N(0) \int_{\Delta}^{\infty} dE \rho(E) I_{qp}(E) \quad (A4)$$

is the total quasiparticle-injection rate. We note that the contributions due to various scattering processes cancel each other. Thus, although the scattering processes affect the quasiparticle distribution, they do not change the quasiparticle number and hence make no contribution to the rate of change of the total quasiparticle density.

Similarly, Eq. (1b), with expression (6) added to account for the phonons escaping from thin films, when summed over all phonon states of energy $\hbar\omega \geq 2\Delta$ gives

$$\begin{aligned} \frac{dN_{ph>}}{dt} = & I_{ph>} - \frac{8\pi N(0)}{\hbar} \int_{3\Delta}^{\infty} dE' \int_{\Delta}^{E'-2\Delta} dE \alpha^2 F(E' - E) \rho(E) \rho(E') \left(1 - \frac{\Delta^2}{EE'}\right) \\ & \times \{f(E)[1 - f(E')]n(E' - E) - f(E')[1 - f(E)][n(E' - E) + 1]\} \\ & - \frac{4\pi}{\hbar} N(0) \int_{\Delta}^{\infty} de \int_{\Delta}^{\infty} dE' \alpha^2 F(E + E') \rho(E) \rho(E') \left(1 + \frac{\Delta^2}{EE'}\right) \\ & \times \{[1 - f(E)][1 - f(E')]n(E + E') - f(E)f(E')[n(E + E') + 1]\} - \frac{N_{ph>} - N_{ph>}^0}{\tau_{es}}, \end{aligned} \quad (A5)$$

where

$$I_{ph>} \equiv \int_{2\Delta}^{\infty} d\Omega NF(\Omega) I_{ph}(\Omega) \quad (A6)$$

is the total phonon injection rate for phonons with energy $\hbar\Omega \geq 2\Delta$. Here we would like to emphasize that the contribution due to the scattering processes that give the first integral term in Eq. (A5) does not vanish. This term is usually ignored.²⁶ However, it should be considered as a source term for the phonons of energy $\hbar\Omega \geq 2\Delta$ when significant amounts of quasiparticles of energy $\hbar\Omega \geq 3\Delta$ are excited. The decay of the quasiparticles with energy $E \geq 3\Delta$ are dominated by scattering process in which phonons are emitted. Therefore, this scattering term can be important when quasiparticles with energy larger than 3Δ are excited.

If the quasiparticle states of energy $E > 3\Delta$ are not significantly disturbed, the scattering contribution in Eq. (A5) can be ignored, and Eqs. (A3) and (A5) can be put into the same form as the RT equations, i.e.,

$$\frac{dN_{qp}}{dt} = I_{qp} - 2RN_{qp}^2 + 2BN_{ph>}, \quad (A7)$$

$$\frac{dN_{ph>}}{dt} = I_{ph>} + RN_{qp}^2 - BN_{ph>} - \frac{N_{ph>} - N_{ph>}^0}{\tau_{es}}, \quad (A8)$$

with

$$\begin{aligned} R & \equiv \frac{4\pi}{\hbar} N(0) \int_{\Delta}^{\infty} dE \rho(E) f(E) \int_{\Delta}^{\infty} dE' \rho(E') f(E') \left[\alpha^2 F(E + E') \left(1 + \frac{\Delta^2}{EE'}\right) [n(E + E') + 1] \right] / N_{qp}^2 \\ & \equiv \left\langle \frac{\pi}{4N(0)\hbar} \alpha^2 F(E + E') \left(1 + \frac{\Delta^2}{EE'}\right) [1 + n(E + E')] \right\rangle_{qp} \end{aligned} \quad (A9)$$

and

$$\begin{aligned} B & \equiv \frac{4\pi}{\hbar} \frac{N(0)}{N} \int_{2\Delta}^{\infty} d\Omega NF(\Omega) n(\Omega) \int_{\Delta}^{\Omega-\Delta} dE \rho(E) \rho(\Omega - E) \alpha^2(\Omega) \left(1 + \frac{\Delta^2}{E(\Omega - E)}\right) [1 - f(E)][1 - f(\Omega - E)] / N_{ph>} \\ & \equiv \left\langle \frac{4N(0)\pi}{\hbar N} \int_{\Delta}^{\Omega-\Delta} dE \rho(E) \rho(\Omega - E) \left(1 + \frac{\Delta^2}{E(\Omega - E)}\right) [1 - f(E)][1 - f(\Omega - E)] \right\rangle_{ph>}, \end{aligned} \quad (A10)$$

where $\langle \dots \rangle_{qp}$ and $\langle \dots \rangle_{ph>}$ represent, respectively, the average over excited quasiparticle pairs and phonon excitations with phonon energy $\hbar\Omega \geq 2\Delta$. We note that both R and B depend upon the steady-state distribution $f(E)$ and $n(\Omega)$. Therefore they vary for different strengths as well as different mechanisms of the driving forces.

APPENDIX B: LINEARIZED ROTHWART-TAYLOR
EQUATIONS

In this appendix we derive the linearized RT equations from the linearized coupled kinetic equations [Eqs. (8a) and (8b)]. We also give comments on the linearized RT equations.

Following the same procedure as was used to derive the RT equations in Appendix A, we obtain from Eq. (8a)

$$\frac{d}{dt}(\delta N_{qp}) = I_{qp} - 2\delta N_{qp} \langle \tau_R^{-1} \rangle'_{qp} + 2\delta N_{ph} \langle \tau_B^{-1} \rangle'_{ph}, \quad (B1)$$

where

$$\langle \tau_R^{-1} \rangle'_{qp} \equiv \int_{\Delta}^{\infty} dE \left(\frac{4N(0)\rho(E)\delta f(E)}{\tau_R(E, T)} \right) / \delta N_{qp} \quad (B2)$$

and

$$\langle \tau_B^{-1} \rangle'_{ph} \equiv \int_{2\Delta}^{\infty} d\Omega \left(\frac{NF(\Omega)\delta n(\Omega)}{\tau_B(\Omega, T)} \right) / \delta N_{ph}. \quad (B3)$$

Here the *excess quasiparticle density* δN_{qp} is defined as

$$\delta N_{qp} \equiv \int_{\Delta}^{\infty} dE 4N(0) \frac{E}{(E^2 - \Delta^2)^{1/2}} [f(E) - f(E, T)]. \quad (B4)$$

We note that this is not the quasiparticle density difference between the driven state and the equilibrium state, because we have used the steady-state energy gap in Eq. (B4) to calculate the quasiparticle density. The *excess phonon density* of phonons with energy $\hbar\Omega \geq 2\Delta$ is defined as

$$\delta N_{ph} \equiv \int_{2\Delta}^{\infty} d\Omega NF(\Omega)\delta n(\Omega). \quad (B5)$$

Similarly, the linearized form of the phonon kinetic equation [Eq. (8b)] gives

$$\frac{d}{dt}(\delta N_{ph}) = I_{ph} + \delta N_{qp} \langle \tau_R^{-1} \rangle'_{qp} - \delta N_{ph}^2 \langle \tau_B^{-1} \rangle'_{ph} - \delta N_{ph} / \tau_{es}. \quad (B6)$$

Here, as discussed in Appendix A, we have neglected contributions from quasiparticle scattering processes [the first term of Eq. (8b)]. Equations (B1) and (B6) differ from the linearized coupled equations derived from Eqs. (A7) and (A8) with R and B fixed as constants. The latter have been applied by Gray to the investigation of the quasiparticle lifetime in Al.⁶ That is, $\langle \tau_R^{-1} \rangle'_{qp}$ differs from $RN_{qp}^0(T)$, where $N_{qp}^0(T)$ is the quasiparticle density in equilibrium state at temperature T and $\langle \tau_B^{-1} \rangle'_{ph}$ differs from B . The difference comes from the fact that both R and B depend upon the steady-state quasiparticle and phonon distributions rather than the equilibrium distributions, and hence cannot be treated as constants.

It follows from Eqs. (B1) and (B6) that in the linearized regime the effective decay rates of the excess quasiparticles and phonons are, respectively, the average recombination times of the *excess* quasiparticles and the average pair-breaking times of the *excess* phonons. The factors of two which appear in Eq. (B1) result from the fact that each event creates or eliminates two quasiparticles.

*Work supported by the Office of Naval Research.

†Preliminary version of this work has appeared [Bull. Am. Phys. Soc. 21, 102 (1976)].

¹D. M. Ginsberg, Phys. Rev. Lett. 8, 204 (1962).

²B. N. Taylor, Ph.D. thesis (University of Pennsylvania, 1963) (unpublished).

³B. I. Miller and A. H. Dayem, Phys. Rev. Lett. 18, 1000 (1967).

⁴K. E. Gray, A. R. Long, and C. J. Adkins, Philos. Mag. 20, 273 (1967).

⁵J. L. Levine and S. Y. Hsieh, Phys. Rev. Lett. 20, 994 (1968).

⁶K. E. Gray, J. Phys. F 1, 290 (1971); I. Schuller and K. E. Gray, Phys. Rev. B 12, 2629 (1975).

⁷L. N. Smith and J. M. Mochel, Phys. Rev. Lett. 35, 1597 (1975).

⁸W. Eisenmenger and A. H. Dayem, Phys. Rev. Lett. 18, 125 (1967).

⁹H. Kinder, K. Lassmann, and W. Eisenmenger, Phys. Lett. 31A, 475 (1970).

¹⁰A. H. Dayem, B. I. Miller, and J. J. Wiegand, Phys. Rev. B 3, 2949 (1971).

¹¹R. C. Dynes, V. Narayanamurti, and M. Chiu, Phys. Rev. Lett. 26, 181 (1971).

¹²A. H. Dayem and J. J. Wiegand, Phys. Rev. B 5, 4390 (1972).

¹³R. C. Dynes and V. Narayanamurti, Phys. Rev. B 6, 143 (1972); Solid State Commun. 12, 341 (1973).

¹⁴A. R. Long and C. J. Adkins, Philos. Mag. 27, 865 (1973).

¹⁵J. Clarke, Phys. Rev. Lett. 28, 1363 (1972); J. Clarke and J. L. Paterson, J. Low Temp. Phys. 15, 491 (1974).

¹⁶A. F. G. Wyatt, V. M. Dmitriev, W. S. Moore, and F. W. Sheard, Phys. Rev. Lett. 16, 1166 (1966).

¹⁷A. H. Dayem and J. J. Wiegand, Phys. Rev. 155, 419 (1967).

¹⁸Yu I. Latyshev and F. Ya. Nad', Zh. Eksp. Teor. Fiz. Pis'ma Red. 19, 737 (1974) [Sov. Phys.-JETP Lett. 19, 380 (1974)]; IEEE Trans. Mag. 11, 877 (1975); D. W. Jillie, J. Lukens, and Y. H. Kao, *ibid.* 11, 671 (1975).

¹⁹V. Narayanamurti and R. C. Dynes, Phys. Rev. Lett. 27, 410 (1971).

²⁰T. C. Tredwell and E. H. Jacobsen, Phys. Rev. Lett. 35, 244 (1975); Phys. Rev. B 13, 2931 (1976).

- ²¹L. R. Testardi, Phys. Rev. B 4, 2189 (1971).
- ²²W. H. Parker and W. D. Williams, Phys. Rev. Lett. 29, 924 (1972).
- ²³P. Hu, R. C. Dynes, and V. Narayanamurti, Phys. Rev. B 10, 2786 (1974).
- ²⁴G. A. Sai-Halasz, C. C. Chi, A. Denenstein, and D. N. Langenberg, Phys. Rev. Lett. 33, 315 (1974).
- ²⁵R. Janik, L. Morelli, N. C. Cirillo, Jr., J.N. Lechevet, W. D. Gregory, and W. L. Goodman, IEEE Trans. Mag. 11, 687 (1975).
- ²⁶A. Rothwarf and B. N. Taylor, Phys. Rev. Lett. 19, 27 (1967).
- ²⁷G. M. Eliashberg, Zh. Eksp. Teor. Fiz. Pis'ma Red. 11, 186 (1970) [Sov. Phys.-JETP Lett. 11, 114 (1970)]; Zh. Eksp. Teor. Fiz. 61, 1254 (1971) [Sov. Phys.-JETP 34, 668 (1972)].
- ²⁸B. I. Ivlev and G. M. Eliashberg, Zh. Eksp. Teor. Fiz. Pis'ma Red. 13, 464 (1971), [Sov. Phys.-JETP Lett. 13, 333 (1971)]; B. I. Ivlev, S. G. Lisitsyn, and G. M. Eliashberg, J. Low Temp. Phys. 10, 449 (1973).
- ²⁹R. A. Vardanyan and B. I. Ivlev, Zh. Eksp. Teor. Fiz. Pis'ma Red. 65, 2326 (1973) [Sov. Phys.-JETP Lett. 38, 1156 (1974)].
- ³⁰C. S. Owen and D. J. Scalapino, Phys. Rev. Lett. 28, 1559 (1972).
- ³¹J. J. Chang and D. J. Scalapino, Phys. Rev. B 9, 4769 (1974); 10, 4047 (1974).
- ³²W. H. Parker, Phys. Rev. B 12, 3667 (1975).
- ³³S. B. Kaplan, C. C. Chi, D. N. Langenberg, J. J. Chang, S. Jafarey, and D. J. Scalapino, Phys. Rev. B (to be published).
- ³⁴J. Bardeen, G. Rickayzen, and L. Tewordt, Phys. Rev. 113, 982 (1959).
- ³⁵J. Bardeen, L. N. Cooper, and J. R. Schrieffer, Phys. Rev. 108, 1175 (1957).
- ³⁶J. J. Chang and D. J. Scalapino, Phys. Rev. Lett. 37, 522 (1976).
- ³⁷J. R. Schrieffer and D. M. Ginsberg, Phys. Rev. Lett. 8, 207 (1962).
- ³⁸M. Tinkham and J. Clarke, Phys. Rev. Lett. 28, 1366 (1972); M. Tinkham, Phys. Rev. B 6, 1747 (1972).
- ³⁹R. Peters and H. Meissner, Phys. Rev. Lett. 30, 965 (1973); I. Schuller and K. E. Gray, *ibid.* 36, 429 (1976); A. Schmid and G. Schön, J. Low Temp. Phys. 20, 207 (1975).
- ⁴⁰R. E. Prange and L. P. Kadanoff, Phys. Rev. 134, A566 (1964).
- ⁴¹D. J. Scalapino, in *Superconductivity*, edited by R. D. Parks (Marcel Dekker, New York, 1969).
- ⁴²R. Stedman, L. Almqvist, and G. Nilsson, Phys. Rev. 162, 549 (1967).
- ⁴³W. L. McMillan and J. M. Rowell, in *Superconductivity*, edited by R. D. Parks (Marcel Dekker, New York, 1969); J. M. Rowell, W. L. McMillan, and R. C. Dynes (unpublished).
- ⁴⁴D. Debye, Ann. Phys. 39, 789 (1912).
- ⁴⁵W. A. Little, Can. J. Phys. 37, 334 (1959).
- ⁴⁶If the microwave photon energy exceeds twice the gap energy, there will be a third term corresponding to the pair-breaking process.
- ⁴⁷See, e.g., J. R. Schrieffer, *Theory of Superconductivity* (Benjamin, New York, 1964).
- ⁴⁸C. Kittel, *Introduction to Solid State Physics*, 4th ed. (Wiley, New York, 1971).
- ⁴⁹I. A. Privorotskii, Sov. Phys.-JETP Lett. 16, 945 (1963); V. M. Bobetic, Phys. Rev. 136, A1535 (1964); J. A. Snow, Phys. Rev. 172, 455 (1968); J. J. Chang and D. J. Scalapino, Phys. Rev. B 9, 4769 (1974).
- ⁵⁰D. C. Mattis and J. Bardeen, Phys. Rev. 111, 412 (1958).
- ⁵¹Here we ignore the branch-imbalance effect which occurs in the electron-injection experiments.
- ⁵²Jhy-Jiun Chang and D. J. Scalapino (unpublished).